

Stratigraphy and Radiolarians of Upper Cretaceous Sedimentary Cover of the Arakapas Ophiolite Massif (Cyprus)

L. G. Bragina and N. Yu. Bragin

Geological Institute, Russian Academy of Sciences, Moscow, Russia

Received February 24, 2004; in final form, September 21, 2005

Abstract—In the basal interval, sedimentary cover of the Arakapas ophiolite massif (southern Cyprus) is composed of metalliferous sediments of the Perapedhi Formation that is divided into three sequences based on diverse radiolarian assemblages. These are basal umbers of the Cenomanian age presumably (2–20 m), inter-layering cherts and umbers of the Turonian–Coniacian (6–10 m), and opoka-like cherts of the Coniacian–Santonian. Higher in the succession, there are olistostrome deposits of the Moni Formation, which unconformably rest on the eroded underlying strata. In this formation also divisible into three sequences, the lower one 200 to 300 m thick is composed of variegated, presumably Campanian silty clays containing olistoliths of basic, presumably Upper Triassic volcanics, Lower Cretaceous sandstones, and opoka-like cherts and cherty limestones of the Albian–lower Cenomanian. Next sequence (100–200 m) is represented by alternation of variegated silty and green bentonitic clays of the Campanian, which enclose frequent olistoliths and horizons of fine-clastic olistostrome breccias. The upper sequence of upper Campanian–lower Maastrichtian bentonitic clays (50–100 m) contains interlayers of ash tuffs and clayey cherty sediments. Carbonate deposits of the upper Maastrichtian–Paleogene, conformably overlie the Moni Formation.

DOI: 10.1134/S0869593806050042

Key words: Cyprus, ophiolites, stratigraphy, Mesozoic, Cretaceous, radiolarians, metalliferous sediments, olistostrome.

INTRODUCTION

A necessary part of research aimed at understanding the structure and geological history of mobile belts is investigation of ophiolite suites and associated rock complexes. One of the latter is sedimentary cover of ophiolitic rocks with basal and lower sequences of metalliferous sediments and olistostromes, which are problematic objects for biostratigraphic analysis. These deposits are commonly dislocated to a considerable extent, having a complicated inner structure, lacking traditional fossils or containing their impoverished assemblages. An additional obstacle is absence of methodical works aimed at the high-resolution stratigraphy of sedimentary formations associated with ophiolites. In this work, our objective was to demonstrate methods and feasibility of relevant stratigraphic analysis using the Upper Cretaceous sedimentary cover of classical ophiolite suites in Cyprus.

The Troodos ophiolite massif of the Cretaceous age in central Cyprus is composed of all rock complexes characteristic of ophiolite suites. The Arakapas fault of sublatitudinal strike in the southern part of the Troodos Ridge is interpreted as an ancient transform fault (Simonian and Gass, 1978). Rocks exposed southward of the fault are attributed to the individual Arakapas ophiolite massif (Fig. 1). Along southern and southwestern flanks of the massif, there are exposed oldest

deposits of ophiolitic sedimentary cover: the Perapedhi Formation (Wilson, 1959) that covers basalts, being represented by metalliferous sediments (umbers and cherts), and the Moni Formation (Pantazis, 1967) corresponding to a classical olistostrome with abundant size-variable olistoliths mostly derived from the Mamonia allochthonous complex of the Mesozoic. The

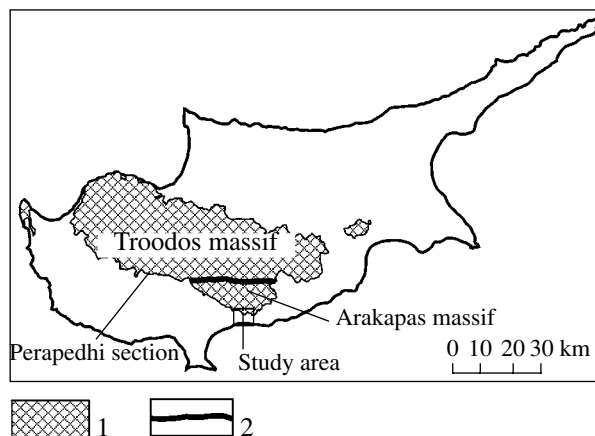


Fig. 1. The Troodos and Arakapas ophiolite massifs of Cyprus: (1) areas of exposed ophiolitic rocks; (2) the Arakapas fault.

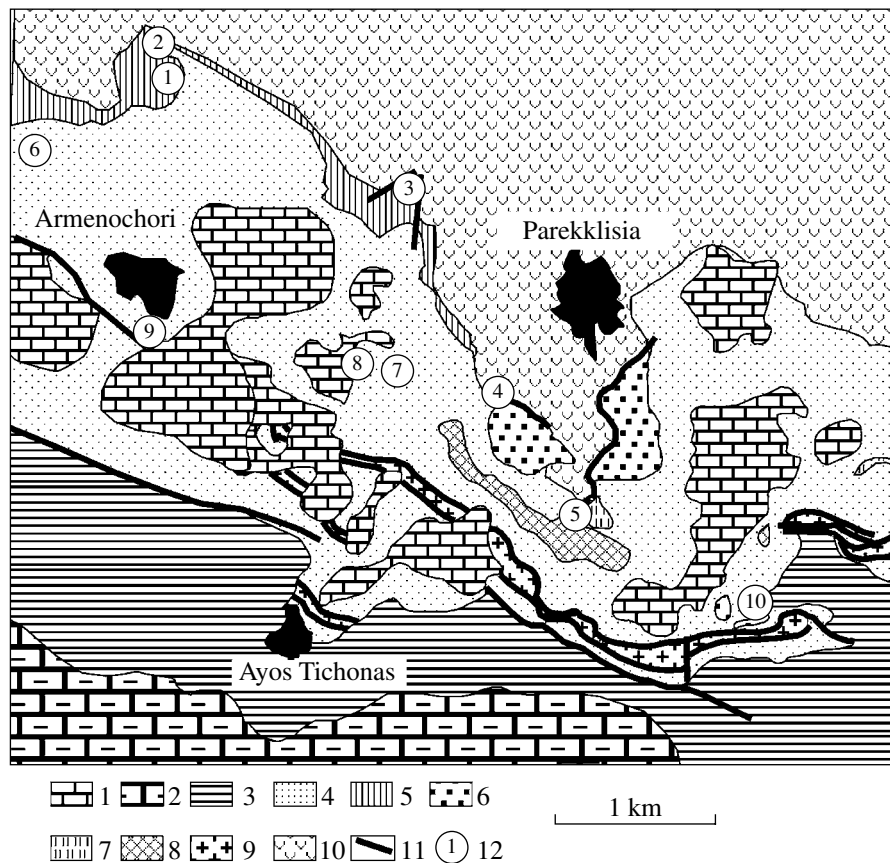


Fig. 2. Schematic geology of the Arakapas massif southern area near the village of Parekklisia (after Urquhart and Robertson, 2000): (1) Koronia Beds, upper Miocene, reefal limestones; (2) Pachna Formation, Miocene, marls and limestones; (3) Lefkara Formation, upper Maastrichtian–Oligocene, marls and limestones; (4) Moni Formation, olistostrome matrix, Campanian–lower Maastrichtian, bentonitic clays; (5) Perapedhi Formation, umbers and cherts, Cenomanian?–Santonian; (6–9) olistoliths in the Moni olistostrome corresponding in lithology to (6) the Parekklisia Beds of the Lower Cretaceous, sandstones, (7) Monagroulli Beds of the Albanian–lower Cenomanian, cherts and cherty limestones, (8) basic volcanics and limestones of the Upper Triassic, and to (9) serpentinites; (10) pillow lavas of the Arakapas massif; (11) faults; (12) numbers of sections described in the text.

last formation is overlain by Maastrichtian–Paleogene deposits of the Lefkara Formation (Fig. 2).

The Perapedhi and Moni formations are practically barren of macrofossils, and only scarce foraminifers are known from these subdivisions. On the other hand, metalliferous sediments, matrix of the Moni olistostrome, and rocks of olistoliths yield abundant and diverse assemblages of radiolarians deserving a careful study. Radiolarians of the Upper Cretaceous have not been studied systematically so far in the areas under consideration, although this group of microfossils is of a considerable stratigraphic potential, as is shown in a series of works on stratigraphy of Triassic, Jurassic, and Cretaceous deposits. The Upper Cretaceous biostratigraphic zonation, the last version of which was published twenty years ago (Sanfilippo and Riedel, 1985), is to be perfected now. In such a situation, the Late Cretaceous radiolarians from Cyprus are of special interest from several viewpoints: they are important in paleontological aspect, since many taxa of potential value for stratigraphy have not been described so far, and in

terms of biostratigraphy (sections of Cyprus with abundant radiolarians offer a possibility to distinguish successive radiolarian zones) and paleobiogeography (Late Cretaceous radiolarians are represented here by assemblages typical of the tropical belt).

PERAPEDHI FORMATION

Along periphery of the Troodos and Arakapas ophiolite massifs, upper pillow lavas and, sometimes, breccias composed of ophiolite-derived clasts (Osozawa and Okamura, 1993) are overlain by metalliferous sediments of the Perapedhi Formation. These sediments of patchy distribution are probably confined to depressions of paleorelief. The formation thickness ranges from dozens centimeters, in the west of island along the Mavrokolimpos River, to dozens meters in the south near the abandoned quarry Mangaleni (Blome and Irwin, 1985; Urquhart and Robertson, 2000). The formation was formerly attributed to the Campanian (Mantis, 1970). Later on, when radiolarians were dis-

covered in umbers of the quarry Mangaleni, Blome and Irwin (1985) suggested the Turonian age of this unit. None of subsequent researchers managed to repeat their discovery (Urquhart and Banner, 1994; Urquhart and Robertson, 2000). At the same time, a diverse assemblage of Santonian–early Campanian radiolarians found within the formation upper part in the Perapedhi stratotype section grounded the idea that the formation base is diachronous (Bragina and Bragin, 1996; Urquhart, Robertson, 2000).

During field work of 2003, we carried out an additional investigation of the Perapedhi Formation in the Mangaleni area, where three sections had been described and sampled. The first one was studied in eastern wall of the quarry Mangaleni, lat. 34°45'23.0" N, long. 33°08'13.1" (section 1, Figs. 2, 3). The rock succession exposed from the base upward at this point is as follows:

1. Dark green to gray–green, sometimes reddish brown basic volcanics displaying often a pillow structure (apparent thickness 10 m).

2. Bright yellow to rusty brown flaggy umbers intercalated with interlayers of brown flaggy and rusty-yellow massive cherts; rocks (Sample 03-13-5) yield radiolarians, which are presumably of Cenomanian age: *Archaeospongoprimum distributum* Bragina, *Alievium sculptus* (Squinabol), *Halesium sexangulum* Pessagno, *Pseudoacanthosphaera magnifica* (Squinabol), *Triactoma fragilis* Bragina, *Dictyodedalus acuticephalus* (Squinabol), *Dictyomitra formosa* Squinabol, *Mita magnifica* Pessagno, *M. sp. B* (Pessagno, 1977), *Pseudodictyomitra nakasekoi* Taketani, *Pseudoecyrtis sp. ex gr. P. pulchra* (Squinabol), *Squinabollum fossile* (Squinabol), *Stichomitra perapedhia* Bragina, *Theocoronium subtriquetrus* Bragina, and *Xitus asymbatos* (Foreman). The unit is 20 m thick.

3. Dark brown thick-flaggy cherts with interlayers of brown siliceous shales; rocks (Sample 03-13-2) yield Turonian radiolarians *Alievium sp. ex gr. A. praegallowayi* Pessagno, *A. superbum* (Squinabol), *Crucella cachensis* Pessagno, *Hexapyramis perforatum* Bragina, *Patulibracchium californiensis* Pessagno, *Pseudoacanthosphaera sp. ex gr. P. superba* (Squinabol), *Pseudoaulophacus lenticulatus* (White), *Quinquecapsularia ombonii* (Squinabol), *Q. sp. ex gr. Q. ombonii* (Squinabol), *Cryptamphorella conara* (Foreman), *B. macropora* Dumitrica, *Diacanthocapsa acuminata* Dumitrica, *D. ancus* Foreman, *D. sp. ex gr. D. euganea* Squinabol, *D. sp. ex gr. D. matsumotoi* (Taketani), *D. rara* Squinabol, *Distylocapsa squama* O'Dogherty, *Doripyle sp. ex gr. D. ovoidea* Squinabol, *Mita sp. A (= Theocampe (?) sp. in Bragina and Bragin, 1996)*, *M. sp. B*, *Pseudodictyomitra sp. A*, *P. sp. B*, *Rhopalosyringium sp. ex gr. R. elegans* (Squinabol), *R. sp. aff. R. adriaticum* O'Dogherty, and *Stichomitra perapedhia* Bragina.

Sample 13-1 collected 1 m higher in the section yielded remains of late Turonian–Coniacian radiolari-

ans: *Alievium sp. ex gr. A. praegallowayi* Pessagno, *A. superbum* (Squinabol), *Archaeospongoprimum distributum* Bragina, *A. sp. ex gr. A. nishiyamae* Nakaseko et Nishimura, *A. sp. A*, *Crucella irwini* Pessagno, *B. messinae* Pessagno, *Falsocromyodrymus ? fragosus* O'Dogherty, *Halesium sexangulum* Pessagno, *Hexapyramis perforatum* Bragina, *Multastrum regalis* Vishnevskaya, *Patulibracchium sp. ex gr. P. teslaensis* Pessagno, *Phaseliforma sp. ex gr. P. ovum* Jud, *Praeconocaryomma sp. ex gr. P. lipmanae* Pessagno, *Pseudoaulophacus lenticulatus* (White), *Ps. venadoensis* Pessagno, *Quinquecapsularia sp. A*, *Q. sp. B*, *Amphipyndax stocki* (Campbell et Clark), *Archaeodictyomitra sp. A*, *Diacanthocapsa ancus* Foreman, *D. antiqua* (Squinabol), *D. sp. ex gr. D. antiqua* (Squinabol), *D. brevithorax* Dumitrica, *D. sp. ex gr. D. euganea* (Squinabol), *D. sp. A*, *Mita sp. A (= Theocampe (?) sp. in Bragina and Bragin, 1996)*, *Pseudodictyomitra sp. A*, *Stichomitra perapedhia* Bragina, *Stichomitra sp. ex gr. S. perapedhia* Bragina, *Thanarla gracilis* (Squinabol), *Ultranapora sp. ex gr. U. durhami* Pessagno, and *Xitus sp. A*. The unit is 9 m thick.

4. Gray-red, pink, and light brown cherts; these Mn-rocks are opoka-like and flaggy, with concentric patterns of secondary silicification, enclosing interlayers of light gray-brown cherty shales. The Coniacian–Santonian radiolarians are detected in the lower part of the bed (Sample 13-4). Their assemblage is represented by *Acaeniotyle diaphorogona* Foreman, *A. macrospina* (Squinabol), *A. umbilicata* (Rust), *Acanthocircus impolitus* O'Dogherty, *A. tympanum* O'Dogherty, *Alievium sp. ex gr. A. praegallowayi* Pessagno, *Archaeospongoprimum bipartitum* Pessagno, *A. distributum* Bragina, *Crucella cachensis* Pessagno, *C. messinae* Pessagno, *Hexapyramis perforatum* Bragina, *Multastrum regalis* Vishnevskaya, *Patulibracchium sp. aff. P. lawsoni* Pessagno, *Praeconocaryomma universa* Pessagno, *Pseudoaulophacus lenticulatus* (White), *P. venadoensis* Pessagno, *Stylosphaera pusilla* Campbell et Clark, *Triactoma compressa* (Squinabol), *T. fragilis* Bragina, *T. micropora* Bragina, *Vitorfus campbelli* Pessagno, *Afens liriodes* Reidel et Sanfilippo, *Annikaella omanensis* De Wever, *Archaeodictyomitra sp. A*, *Bathropyramis sp. A*, *Cornutella californica* Campbell et Clark, *Dictyomitra formosa* Squinabol, *Microsciadiocapsa madisonae* Pessagno, *M. sutterensis* Pessagno, *Mita magnifica* Pessagno, *M. sp. A (= Theocampe (?) sp. in Bragina and Bragin, 1996)*, *M. sp. B* (Pessagno, 1977), *M. sp. B*, *M. sp. D (= Stichomitra (?) sp. in Bragina and Bragin, 1996)*, *Pseudodictyomitra nakasekoi* Taketani, *P. sp. A*, *P. sp. B*, *Rhopalosyringium sp. aff. R. adriaticum* O'Dogherty, *Stichomitra perapedhia* Bragina, *Theocampe (?) cypraea* Bragina, and *Theocoronium subtriquetrus* Bragina (apparent thickness is 6 m).

In the northern wall of the quarry (section 2, lat. 34°45'27.2" N, long. 33°08'07.1"), deposits of the Perapedhi Formation are of similar lithologic composition being less thick however. The rock succession

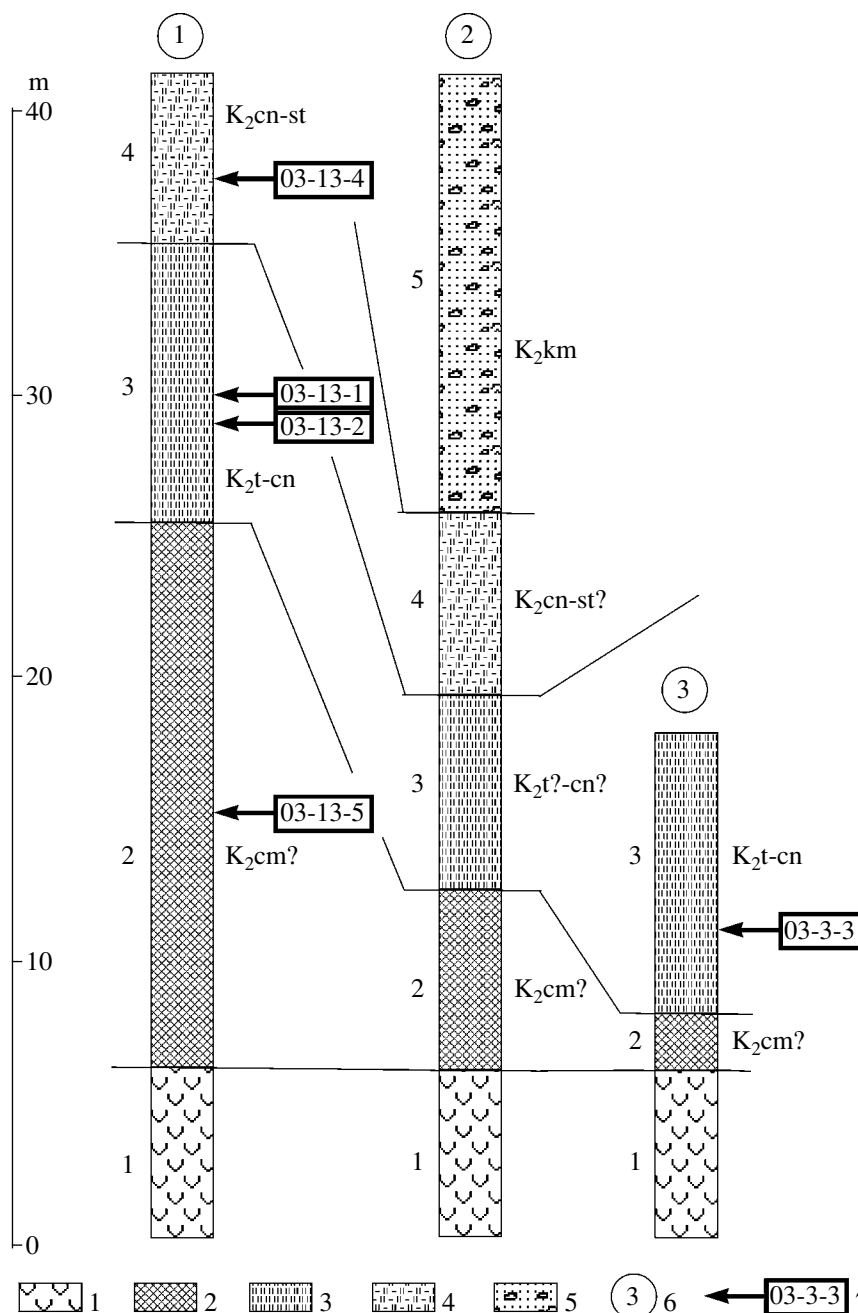


Fig. 3. Lithostratigraphy of the Perapedhi Formation in the abandoned quarry Mangaleni (bed number and age are indicated to the left and right of the columns, respectively): (1) basic volcanics; (2) umbers; (3) cherts; (4) opoka-like cherts; (5) olistostrome; (6) section number; (7) sampling level and sample number.

exposed here (Figs. 2, 3) is as follows (from the base upward):

1. Basic volcanics (apparent thickness 1 m).
2. Umbers dark brown, siliceous and massive, alternating with yellow flaggy umbers (thickness 6 m).
3. Dark brown cherts and umbers, flaggy and thin-bedded (thickness 6 m).
4. Pink and light gray opoka-like Mn-cherts (thickness 6 m).

5. Gray bentonitic clays with abundant small (up to 1 m across) blocks of gray cherts (apparent thickness 15 m).

Bed 5 of the section 2 belongs already to the overlying Moni Formation.

One more section of the Perapedhi Formation has been described 1.5 km to the east-southeast of the quarry Mangaleni (section 3, lat. 34°45'04.6" N, long.

33°08'50.8" E). The rock succession exposed here (Figs. 2, 3) is as follows:

1. Basic volcanics (apparent thickness 2 m).
2. Dark brown massive umbers with interlayers of yellow–brown cherts (thickness 2 m).
3. Dark brown loose thin-bedded umbers with interlayers of dark brown flaggy cherts, containing Fe–Mn nodules. Rocks (Sample 03-3-3) yield radiolarians of the upper Turonian?–Coniacian. The radiolarian assemblage consists of *Acanthocircus venetus* (Squinabol), *Acaeniotyle macrospina* (Squinabol), *A. sp. ex gr. A. starka* Empson–Morin, *Alievium sp. ex gr. A. superbum* (Squinabol), *A. sp. ex gr. A. murphyi* Pessagno, *Archaeospongoprimum distributum* Bragina, *Cruccella cachensis* Pessagno, *C. messinae* Pessagno, *Falsocromyodrymus sp. cf. F. mirabilis* (Squinabol), *Halesium sexangulum* Pessagno, *Multastrum regalis* Vishnevskaya, *Patulibracchium sp. ex gr. P. teslaensis* Pessagno, *Phaseliforma inflata* Bragina, *Pseudoaulophacus lenticulatus* (White), *P. venadoensis* Pessagno, *Pseudoacanthosphaera magnifica* (Squinabol), *Quinquecapsularia ombonii* (Squinabol), *Q. sp. A*, *Stylodictya insignis* Campbell et Clark, *Triactoma fragilis* Bragina, *Vitorfus sp. A* (Pessagno, 1977), *Afens liriodes* Reidel et Sanfilippo, *Amphipyndax stocki* (Campbell et Clark), *Archaeodictyomitra sp. A*, *Coniforma sp. ex gr. B. antiochensis* Pessagno, *Cornutella californica* Campbell et Clark, *Cryptamphorella conara* (Foreman), *B. sphaerica* (White), *Diacanthocapsa brevithorax* Dumitrica, *Diacanthocapsa sp. ex gr. D. ancus* (Foreman), *Diacanthocapsa sp. ex gr. D. rara* Squinabol, *Dictyomitra formosa* Squinabol, *Distylacapsa squama* O'Dogherty, *Microsciadiocapsa radiata* Pessagno, *M. sp. ex gr. M. radiata* Pessagno, *Mita sp. A (Theocampe (?) sp.* (Bragina and Bragin, 1996), *M. sp. B* (Pessagno, 1977), *Petasisforma (?) inusitata* Pessagno, *Pseudodictyomitra nakasekoi* Taketani, *P. sp. ex gr. P. nakasekoi* Taketani, *P. sp. A*, *Rhopalosyringium sp. aff. R. adriaticum* O'Dogherty, *Rotaforma volatilis* O'Dogherty, *Sciadiocapsa euganea* (Squinabol), *Stichomitra perapedhia* Bragina, *Theocampe sp. A*, *T. sp. cf. T. tina* (Foreman), *Turbocapsula sp. ex gr. T. giennensis* O'Dogherty, *Ultranapora sp. A*, *Ultranapora sp. ex gr. U. durhami* Pessagno, 1977, and *Xitus sp. A* (apparent thickness 10 m).

Our investigation confirmed the three-member structure of the Perapedhi Formation in sections of the Mangaleni area that was established earlier (Urquhart and Robertson, 2000). The lower sequence that is presumably of the Cenomanian Stage is composed predominantly of umbers and ranges in thickness from 2 to 20 m. The middle sequence of alternating chert and umber beds (6–10 m thick in total) corresponds in age to the Turonian–Coniacian, and the upper one represented by opoka-like cherts is of the Coniacian–Santonian age (thickness 6 m). Our dating results differ from those of predecessors who attributed the umber sequence to the Turonian Stage (Blome and Irwin, 1985).

MONI FORMATION

To the south and southeast of the Arakapas massif, olistostrome sequence distinguished as the Moni Formation overlies the Perapedhi Formation or rests directly on basalts of ophiolite suite in many places (Pantazis, 1967). Blocks of diverse rocks or olistoliths of the sequence are included into bentonitic clay matrix. They range in dimensions from a few centimeters to 1.5 km across. Small and large olistoliths are mostly composed of rocks of the allochthonous complex Mamonia, which are widespread in the southwestern Cyprus. These are Triassic basic volcanics with interlayers of micritic limestones, Jurassic cherts, jaspers and limestones, and Lower Cretaceous sandstones, cherts and cherty shales. In addition, there are known blocks of serpentinites and basic volcanics, which are derived from the Arakapas ophiolite massif, and blocks of umbers and cherts belonging to the Perapedhi Formation. Based on radiolarians occurring in the matrix, the Moni Formation is attributed to the Campanian (Urquhart and Banner, 1994; Urquhart and Robertson, 2000), but microfauna of the formation has not been studied systematically so far. In the westerly areas of Cyprus, facies analogues of the Moni olistostrome are (1) the Kannaviou Formation (Campanian) of bentonitic clays (Swarbrick and Robertson, 1980; Urquhart and Banner, 1994; Bragina and Bragin, 1995) and (2) the Kathikas Formation (uppermost Campanian–lower Maastrichtian) of sedimentary breccias of gravity genesis with bentonitic clay and marl interlayers (Swarbrick and Robertson, 1980; Urquhart and Banner, 1994; Bragina and Bragin, 1995). Being in the same stratigraphic position, these facies analogues are, like the Moni Formation, the components of the Upper Cretaceous sedimentary cover of the Troodos ophiolites. Origin of the Moni olistostrome is assumed to be related to collision of the allochthonous complexes Troodos and Mamonia (Swarbrick and Robertson, 1980; Urquhart and Robertson, 2000). In the present-day structure of Cyprus, the composite nappe of the Mamonia Complex is thrust over the Troodos ophiolites. During the thrusting of the Campanian–Maastrichtian time, products of destruction of the Mamonia nappe front have been included as blocks into the Moni olistostrome and are dominant therefore among olistoliths.

We studied several sections of the Moni Formation in order to subdivide it into subunits, to establish the matrix age with a higher resolution, and to obtain new data on geological relations and origin of this formation. Beyond the quarry Mangaleni, the formation lower part is exposed near the village of Parekklesia, where it rests directly on ophiolites. Southwestward of the village, we observed the following section (section 4, lat. 34°44'10.6" N, long. 33°09'11.7" E; Figs. 2, 4):

1. Green brecciated pillow lavas with intercalation of reddish yellow hyaloclastites (apparent thickness 5 m).

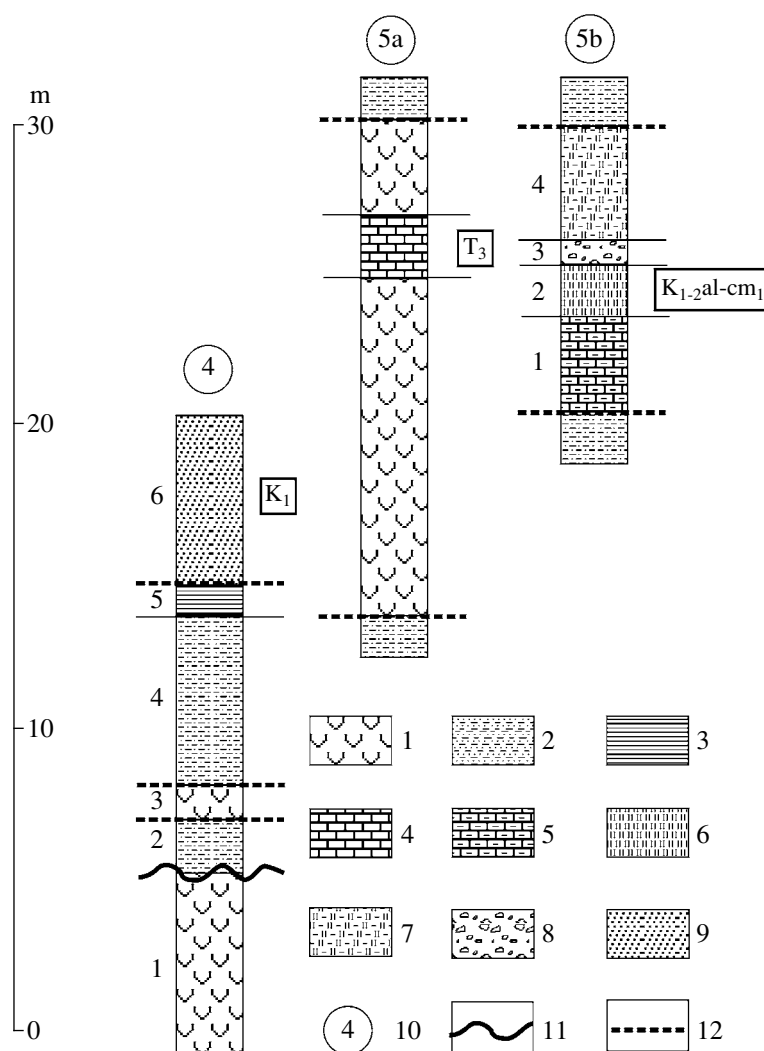


Fig. 4. Lithostratigraphy of the Moni Formation lower sequence and some olistoliths (bed number and age are indicated to the left and right of the columns, respectively): (1) basic volcanics; (2) silty clay; (3) bentonitic clay; (4) limestone; (5) cherty limestone; (6) chert; (7) opoka-like chert or cherty shale; (8) cherty-carbonate breccia; (9) sandstone; (10) section number; (11) unconformity; (12) outer boundaries of olistoliths.

2. Brown to greenish silty clays with interlayers of black Fe-Mn cherty shales and rare intercalations of brick-red siltstones (thickness 5 m).

3. Gray-green bentonitic clays (thickness 1 m).

4. A large block (olistolith) of yellowish gray massive quartz sandstone (apparent thickness up to 20 m).

Clays of Bed 2 contain redeposited radiolarians of the Lower Cretaceous: *Holocryptocanium barbui* Dumitrica, *Pseudodictyomitra carpatica* (Loznyiak), and *Thanarla conica* (Aliev). It is logical to suggest that their appearance in the bed is a result of redeposition from the Lower Cretaceous clays known in the lower part of the Mamonia Complex that was the main source of olistoliths. The Lower Cretaceous and Albian-Turonian deposits in the upper part of the Mamonia Complex are represented by red clay (80–90%) sometimes bearing radiolarians (Bragin et al.,

2000). Sliding into the basin, where the Moni Formation accumulated, blocks of that clay disintegrated quickly, and their material became mixed with the matrix (bentonitic clay). This is an explanation for appearance of brown and reddish interlayers in green bentonite and for enrichment of the latter in silty and sandy fraction.

These variegated silty clays of mixed composition are most characteristic of lower and middle parts of the Moni Formation, where olistoliths are mostly concentrated. The largest olistoliths exposed southward of the village of Parekklesia (Fig. 2) are composed of quartz-polymictic sandstones of the lower Cretaceous (Parekklesia Beds) or of opoka-like cherts and cherty limestones attributed to the Monagroulli Beds of the Albian-Cenomanian (Swarbrick and Robertson, 1980) and of basic volcanics belonging to the Mamonia Complex. Radiolarians occur nearly in all the blocks (except

for sandstones of the Parekklesia Beds) and, being studied in detail, they offer a possibility to obtain new data on age of their host rocks.

We studied two large blocks located southward of the village of Parekklesia. One olistolith extending for the distance of about 1.5 km and up to 200 m thick is composed of green, red-brown and dark gray altered basic volcanics, which are frequently amygdaloidal, displaying sometimes the pillow structure (Figs. 2, 4). Lenticular bodies of pink and gray micritic limestones intercalated with volcanics yield radiolarians of the Upper Triassic. Species identified in one of the limestone lenses (section 5, lat. 34°43'49.9" N, long. 33°09'37.9" E) are *Capnuchosphaera silviesensis* Blome, *B. sp. cf. B. concava* De Wever, *C. sp. cf. C. theloides* De Wever, *Pseudostylosphaera sp. cf. P. hellenica* (De Wever), *Spongostylus carnicus* Kozur et Mostler, *Vinassaspongus sp. cf. V. subsphaericus* Kozur et Mostler and others of the late Carnian-early Norian age.

The other block (section 5b, lat. 34°43'56.5" N, long. 33°09'37.1" E) is composed of cherty-carbonate rocks of the Monagroulli Beds formerly attributed to the Cenomanian-Turonian (Urquhart and Robertson, 2000), but we dated them otherwise. In the block of the Monagroulli Beds exposed in a roadway excavation (Figs. 2, 4), we observed the following units (north-to-south succession):

1. Interlayering of gray cherty limestones, gray radiolarian cherts, light gray cherty marls and breccias of small chert and limestone fragments (apparent thickness 2 m).

2. Unexposed interval (1 m) and pink opoka-like flaggy cherts with interlayers of red radiolarian clayey jasper (thickness 2 m).

3. Chert-limestone breccia (thickness 1 m).

4. Interlayering of gray porous opoka-like cherts and gray calcareous clays (apparent thickness 3 m).

A greater part of this olistolith is poorly exposed. Detrital material in many places is represented by rocks observable in the above excavation, e.g., by pink or yellowish pink and gray opoka-like porous radiolarian cherts, chert-limestone breccia, rarer marls and red radiolarian jasper. Abundant and diverse radiolarians frequently occur in these rocks. In pink chert from the lower part of Bed 2 described above (Sample 03-2), we determined very diverse species of Albian radiolarians. These are *Acaeniotyle diaphorogona* Foreman, *A. macrospina* (Squinabol), *A. tribulosa* Foreman, *Acanthocircus venetus* (Squinabol), *Archaeocenosphaera ? mellifera* O'Dogherty, *Becus horridus* (Squinabol), *Dactyliodiscus lenticulatus* (Jud), *Falsocromyodrymus mirabilis* (Squinabol), *Quinquecapsularia sp. ex gr. Q. ombonii* (Squinabol), *Q. sp. ex gr. Q. panacea* O'Dogherty, *Staurosphaeretta longispina* (Squinabol), *Triactoma paronai* (Squinabol), *Crolanium sp. ex gr. C. pulchrum* (Squinabol), *C. spineum* (Pessagno), *Dicatomytra obesa* (Squinabol), *Mita magnifica* Pessagno,

Novixitus mclaughlini Pessagno, *Obeliscoites perspicuus* (Squinabol), *O. turris* (Squinabol), *Pseudodictyomitra pseudomacrocephala* (Squinabol), *Rhopalosyringium euganeum* (Squinabol), *R. mosquense* (Smirnova et Aliev), *Spongocapsula (?) zamoraensis* (Pessagno), *Thanarla gracilis* (Squinabol), *T. praevienta* Pessagno, *B. pulchra* (Squinabol), *B. spoletensis* O'Dogherty, *Torculum coronatum* (Squinabol), *Tugurium pagoda* (Squinabol), *Ultranapora durhami* Pessagno, *U. praespinifera* Pessagno, *U. spinifera* Pessagno, and *U. sp. A.*

In the upper part of Bed 2 (Sample 03-2 collected 20 cm higher in the section), the identified early Cenomanian radiolarians are represented by *Acaeniotyle glebulosa* (Foreman), *A. macrospina* (Squinabol), *Alievium sp. ex gr. A. sculptus* (Squinabol), *Archaeospongoprimum sp. cf. A. archaeobipartitum* Bragina, *Becus horridus* (Squinabol), *B. regius* O'Dogherty, *Crucella euganea* (Squinabol), *Dactyliosphaera silviae* Squinabol, *Halesium sexangulum* Pessagno, *Patellula sp. ex gr. P. spica* O'Dogherty, *Pessagnobrachia sp. ex gr. P. irregularis* (Squinabol), *Phaseliforma sp. ex gr. P. laxa* Pessagno, *Protoxiphotractus sp. A.*, *Pseudocanthosphaera sp. ex gr. P. spinosissima* (Squinabol), *Quinquecapsularia sp. ex gr. Q. ombonii* (Squinabol), *Staurosphaeretta sp. ex gr. S. grandipora* (Squinabol), *Amphipyndax stocki* (Campbell et Clark), *Novixitus dengoi* Schmidt-Effing, *Obeliscoites sp. ex gr. O. maximus* (Squinabol), *Pseudodictyomitra sp. ex gr. P. nakasekoi* Taketani, *P. pseudomacrocephala* (Squinabol), *Rhopalosyringium elegans* (Squinabol), *Squinabollum fossile* (Squinabol), *Stichomitra sp. ex gr. S. insignis* Squinabol, *Thanarla sp. ex gr. T. conica* (Squinabol), *T. elegantissima* (Cita), *T. veneta* (Squinabol), and *Torculum coronatum* (Squinabol).

Thus, olistoliths are concentrated mostly in the lower sequence of the Moni Formation, where matrix composed largely of variegated clay contains redeposited radiolarians of the Lower Cretaceous. It is likely that the Moni Formation rests discordantly on underlying deposits, because it contains olistoliths of the Perapedhi Formation rocks and metalliferous sediments of the Perapedhi Formation pinch out in a series of sections. The lower sequence is most likely of the Campanian age, although this should be proved by paleontological evidence; it is from 200 to 300 m thick.

The middle interval of the Moni Formation has been observed in the quarry under mining that is located 1.5 km southwestward of the village of Armenochori (Figs. 2, 3, section 6, lat. 34°45'09.6" N, long. 33°07'10.5" E). The rock succession in this section is as follows (from the base upward):

1. Greenish gray bentonitic clay; the rock is thin-bedded flaggy, containing interlayers (up to 0.5 m thick) of greenish gray compact silty clay (apparent thickness 6.5 m).

2. Greenish gray bentonitic clay with interlayers of reddish brown silty clay and gray aleurite (thickness 5.5 m).

3. Olistostrome horizon with small (30–40 cm across) subangular fragments of jasper, serpentinite and sandstone (thickness 1.5 m).

4. Greenish gray bentonitic clay with interlayers of greenish gray silty clay and rare blocks (0.5 × 0.5 m) of gray sandstone (thickness 4 m).

5. Greenish gray bentonitic clay and intercalations of red-brown clay containing frequent small olistoliths (thickness 5 m).

6. Greenish dark gray bentonitic clay with frequent olistoliths, some of which represent blocks of chert-carbonate breccias derived from the Monagroulli Beds (thickness 7 m).

7. Dark gray and greenish brown bentonitic clays (thickness 4 m).

8. Greenish and reddish brown silty bentonitic clays with abundant small olistoliths (thickness 10 m).

9. Olistostrome horizon with abundant small olistoliths (thickness 1 m).

10. Greenish brown, yellowish and greenish gray bentonitic clays (thickness 6 m).

It is obvious that variegated clays grade upward in this section into more typical bentonite almost lacking olistoliths. A similar situation has been observed in the other section located 1.3 km westward of the village of Parekklisia, where transition from the middle to upper interval of the Moni Formation is recorded (Section 7 from the base at lat. 34°44'15.5" N and long. 33°08'7.6" E to the top at lat. 34° 44'19.1" N and long. 33°08'52.7" E). The rock succession is as follows:

1. Red silty clay with interlayers of green and greenish gray clays; abundant olistoliths (up to 2 m across) are represented by diverse rocks, the yellow-brown cherts and umbers included (apparent thickness over 50 m).

2. Red-gray to red silty clays with interlayers of greenish gray bentonitic clay scarce small olistoliths (thickness 11 m).

3. Gray-green to gray or yellowish gray bentonitic clays; these flaggy thin-bedded clay contain rare small olistoliths of gypsic cherts. Radiolarian species identified in Sample 03-6-3 are *Alievium praegallowayi* Pessagno, *Cromyodruppa concentrica* Lipman, *Pentinastrum subbotinae* Lipman, *Pseudoaulophacus parguerensis* Pessagno, *P. riedeli* Pessagno, *Pyramispongia glascocensis* Pessagno, *Afens liriodes* Reidel et Sanfilippo, *Archaeodictyomitra lamellicostata* (Foreman), *Podocapsa* (?) *topferia* Empson-Morin, *Diacanthocapsa antiqua* (Squinabol), *D. elongata* Bragina (in litt), *D. sp.* ex gr. *D. fossilis* (Squinabol), *Lithocampe eureia* Foreman, *Rhopalosyringium sp. A*, *Theocampe sp.* ex gr. *T. comprimerta* Empson-Morin, and *Xitus asym-batos* (Foreman). Bed is 4.5 m thick.

4. Olistostrome horizon with abundant unsorted clasts and block (up to 1 × 1 m in size) of cherty limestones, cherts and quartz sandstones (thickness 1.5 m).

5. Red-brown silty gypsiferous clay with ferruginate patches and olistoliths of cherts (thickness 1.5 m).

6. Gray-green bentonitic clay with abundant small olistoliths of sandstones and cherts; clay contains radiolarians of the upper Campanian and Maastrichtian, most probably of the lower Maastrichtian. Species identified in Sample 03-6-2 are *Alievium gallowayi* (White), *A. praegallowayi* Pessagno, *A. vielseitigus* Empson-Morin, *Amphisphaera sp.* ex gr. *A. aotea* Hollis, *Archaeocenosphaera ? mellifera* O'Dogherty, *Archaeospongoprimum nishiyamae* Nakaseko et Nishimura, *A. salumi* Pessagno, *Cromyodruppa concentrica* Lipman, *Crucella aster* (Lipman), *B. latum* (Lipman), *Hexapyramis sp.* cf. *H. perforatum* Bragina, *Lithospilus sp.* ex gr. *L. coronatus* Squinabol, *Paronaella tumida* (Lipman), *Patellula euessceei* Empson-Morin, *P. verteroensis* (Pessagno), *Phaseliforma carinata* Pessagno, *P. laxa* Pessagno, *P. subcarinata* Pessagno, *Porodiscus sp. A*, *Praeconocaryomma universa* Pessagno, *P. sp.* ex gr. *P. lipmanae* Pessagno, *Protoxi-photractus sp.* ex gr. *P. wilsoni* Hollis, *Pseudoaulophacus floresensis* Pessagno, *P. lenticulatus* (White), *Ps. parguerensis* Pessagno, *P. praefloresensis* Pessagno, *P. riedeli* Pessagno, *Spongodiscus sp.* ex gr. *S. rhabdostylus* (Ehrenberg), *Stylosphaera sp.* ex gr. *S. hastata* Campbell et Clark, *Afens liriodes* Reidel et Sanfilippo, *Amphipyndax sp.* ex gr. *A. pseudoconulus* (Pessagno), *A. stocki* (Campbell et Clark), *A. sp.* ex gr. *A. stocki* (Campbell et Clark), *A. tylotus* Foreman, *Artostrobium urna* Foreman, *Bisphaerocephalina* (?) *herox* (Campbell et Clark), *Clathropyrgus tithium* Reidel et Sanfilippo, *Cryptamphorella macropora* Dumitrica, *Diacanthocapsa sp.* ex gr. *D. brevithorax* Dumitrica, *Dictyomitra densicostata* Pessagno, *D. sp.* ex gr. *D. densicostata* Pessagno, *D. formosa* Squinabol, *D. sp. A*, *Lithocampe eureia* Foreman, *Lithocampe sp.* ex gr. *L. eureia* Foreman, *Podocapsa* (?) *topferia* Empson-Morin, *Rhopalosyringium sp.* ex gr. *R. magnificum* Campbell et Clark, *Siphocampe daseia* (Foreman), and *Xitus asym-batos* (Foreman). Bed is 2.5 m thick.

7. Gray-green grumous nonlaminated bentonitic clay with patches of Fe and Mn hydroxides (thickness 3.5 m).

8. White to yellowish gray massive reefal limestones of the upper Miocene corresponding to the Koronia beds of the Pachna Formation (thickness 20 m).

Beds 3–7 belong to the upper part of the Moni Formation. As for the middle part of the latter, it corresponds to a sequence of alternating variegated silty and green bentonitic clays with frequent olistoliths and horizons of small-clastic olistostrome breccias. Being 100 to 200 m thick, the sequence is of the Campanian age presumably.

The upper part of the Moni Formation has been studied in four sections, one corresponding to Section 7

described above. Higher beds of this interval have been studied 0.5 km southwestward of the Section 7 terminal point (Section 8, lat. 34°44'17.6" N, long. 33°08'37.7" E, Figs. 2, 5). Beds exposed here are composed of the following rocks:

1. Gray-green bentonitic clay with rare chert olistoliths and interlayers of gray cherty ash tuff (apparent thickness 6 m).

2. Brown-gray silty clay (thickness 1 m).

3. Gray compact bentonitic clay intercalated with greenish gray foliated clay (thickness 3.5 m).

4. Gray to greenish gray bentonitic clay with boudinage horizons of gray clayey cherts; according to oral communication of O.A. Korchagin, the foraminiferal assemblage in the rock consists of *Gansserina* sp. cf. *G. gansseri* (Bolli), *Globotruncanita stuarti* (de Laparent), *Planohedbergella* (?) *praeiehilensis* (Pessagno), *Globocarinata cretacea* (d'Orbigny), *Rugotruncana subcircumnodifer* (Gandolfi), *Globotruncanella havanensis* (Voorwijk), *Pseudotextulariella elegans* (Rhenak), *Pseudoguembelina costulata* (Cushman), and *Heterohelix navarroensis* Loeblich (O.A. Korchagin, private communication). The thickness is 2 m.

5. White and light yellowish gray massive reefal limestone referred to the upper Miocene (Koronna Beds, Pakhna Formation). The thickness is 30 m.

In this small outcrop, there are interlayers of ash tuff and cherts first appearing in the Moni Formation sequence, and clays exhibit distinct bedding. The upper part of the Moni Formation is quite similar in lithology to the Campanian–lower Maastrichtian Kannaviou Formation of western Cyprus, where it is composed of bentonitic clay being deprived of olistoliths however. A similar section has been observed 1 km south-southwestward of the village of Armenochori (Section 9, lat. 34° 44' 17.6" N, long. 33° 08' 37.7" E, Figs. 2, 5). The following rocks are exposed here (from the base upward):

1. Greenish gray bentonitic clay grading into reddish brown silty clay with frequent small olistoliths of cherts and basic volcanics (apparent thickness 15–20 m); the next interval up to 10 m thick is unexposed.

2. Greenish gray flaggy bentonitic clay with interlayers of gray cherty shale (apparent thickness 2 m); the next interval 5 m thick is unexposed.

3. Greenish to light gray bentonitic flaggy laminated clays with thin (1 cm) black Mn-enriched laminae (apparent thickness 5 m).

4. Light gray thick-platty to massive ash tuff (thickness 2 m).

5. Greenish to gray flaggy bentonitic clay (thickness 2 m).

6. Olistostrome horizon with small clasts of basalt and chert (thickness 1.5 m).

7. Greenish gray to gray flaggy bentonitic clay with interlayers of greenish gray cherty shale (thickness 7 m).

After unexposed interval of 15 m, there are observable outcrops of the Lefkara Formation marls (upper Maastrichtian–Paleogene).

We observed contact between the Moni and Lefkara formations in one section only, where large olistoliths are present in the upper part of the Moni Formation. This section is situated 2.5 km southwestward of the village of Pyrgos (Section 10, lat. 34°43'40.3" N, long. 33°10'08.1" E, Figs. 2, 5). The following beds are exposed here (from the base upward):

1. Gray, yellow and red-brown massive medium-grained quartz sandstones with ferruginate nodules; rocks correspond to a large block of the Perekklisia Beds, which is over 50 m long (apparent thickness 10 m).

2. Greenish brown and greenish gray laminated bentonitic clays with sandstone blocks up to 1 × 1 m in size (thickness 8 m).

3. White to light gray flaggy marls (thickness 2 m).

4. Interlayering of light gray marls and pink-gray calcareous cherts (apparent thickness 1.5 m).

Beds 3 and 4 of this section belong to the basal part of the Lefkara Formation that spans stratigraphic interval from the upper Maastrichtian to Oligocene. There is no sign of unconformity at the contact of beds 2 and 3. The upper sequence of the Moni Formation is composed predominantly of bentonitic clays with interlayers of clayey chert or cherty shale, ashy tuff and olistostrome breccia; olistoliths are rare. The described sequence spans interval from the upper Campanian to lower Maastrichtian, inclusive. It can be as thick as 50 to 100 m.

Thus, general stratigraphic scheme of the Upper Cretaceous sediments covering the Arakapas ophiolite massif (Fig. 6) includes the Perapedhi Formation of three-member structure with lower (Cenomanian), middle (Turonian–Coniacian) and upper (Coniacian–Santonian) sequences, which are capped by the Moni Formation also divisible into three sequences: the lower and middle ones corresponding to the Campanian and the upper one of the Campanian–Maastrichtian age. The Moni Formation overlies with signs of erosion the underlying deposits; hiatus between the Perapedhi and Moni formations may correspond to a part of the Santonian Stage. Sediments assumed to be of the upper Maastrichtian age rest conformably on the upper sequence of the Moni Formation.

CRETACEOUS RADIOLARIAN ASSEMBLAGES OF PERAPEDHI AND MONI FORMATIONS

Among radiolarians from the lower sequence of the Perapedhi Formation (Section 1, Bed 2, Sample 13-5), there are species of wide stratigraphic ranges. For instance, *Mita magnifica* existed in the Albian–Turonian time; *Alievium sculptus* (Squinabol) and *Dictyodetalus acuticephalus* (Squinabol) are characteristic of the Albian–Cenomanian (Bragina, 1999, 2001, 2004;

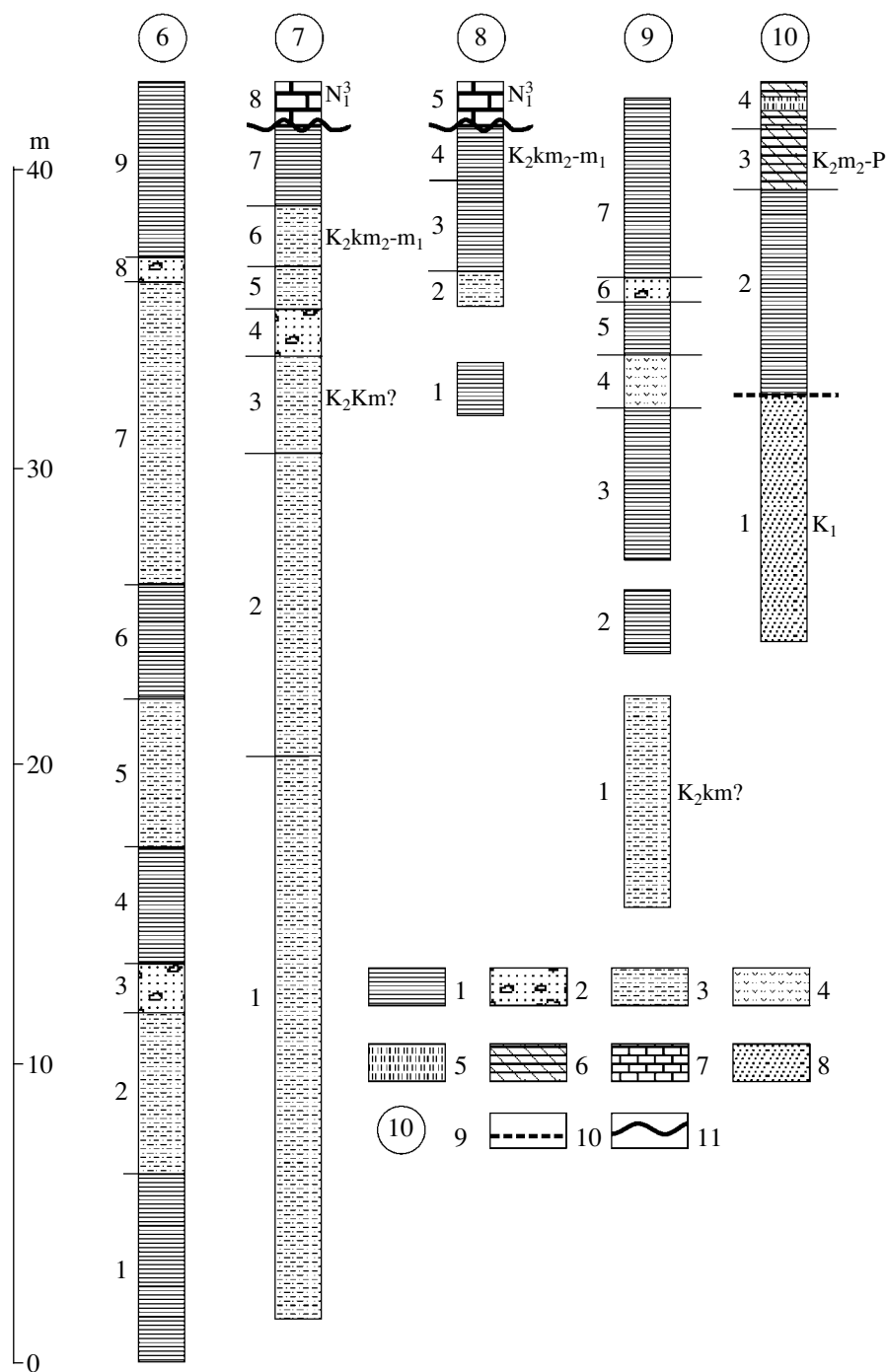


Fig. 5. Lithostratigraphy of the Moni Formation upper sequence (bed number and age are indicated to the left and right of the columns, respectively): (1) bentonitic clay; (2) olistostrome breccia; (3) silty clay; (4) ashy tuff; (5) chert; (6) marl; (7) limestone; (8) sandstone; (9) section number; (10) outer boundaries of olistoliths; (11) unconformity.

O'Dogherty, 1994); *Squinabollum fossile* of the Cenomanian–Santonian; *Halesium sexangulum* and *Dictyomitra Formosa* of the Cenomanian–Campanian. The assemblage is lacking *Doripyle ? anisa* that is index species of upper subzone of the upper Albian *Thanarla spoletensis* Zone in radiolarian zonation of the Mediterranean region (O'Dogherty, 1994); some other spe-

cies, which ceased to exist in the Albian are also missing from the assemblage. Consequently, the assemblage could be of the Cenomanian age not older. As the assemblage is lacking *Alievium superbum*, the index species of synonymous Turonian zone in circum-tropical areas (Pessagno, 1976), and some other species characteristic of the Turonian, we suggest that it is not

younger than the Cenomanian. The *Dactyliosphaera silviae* Zone corresponding in the Mediterranean zonation to the Cenomanian without its very basal interval consists of the lower *Patellula spica* and upper *Guttacapsa biacuta* subzones. Both index species have not been found however among the studied radiolarians, and their assemblage can be restricted in age by the Cenomanian Stage, being unsuitable for a more precise dating.

Radiolarians from middle sequence of the Perapedhi Formation (Section 1, Bed 3, samples 13-2 and 13-1; Section 3, Bed 3, Sample 3-3) are more diverse, enabling dating of a higher resolution. In majority, species identified in Sample 13-2 are characteristic of Cenomanian and Turonian stages. *Alievium superbum* present in the assemblage is index species of synonymous Turonian zone (Pessagno, 1976) and constrains the Turonian age of radiolarians from this sequence.

In Sample 13-1, species characteristic of the Cenomanian and Turonian, which are mostly inherited from the previous assemblage, occur in association with forms not occurring below. The assemblage from this sample includes *Alievium superbum*, the index species of synonymous Turonian zone. It is known, however, that this species existed in the Coniacian as well (Pessagno, 1972). The assemblage also includes *Pseudoaulophacus venadoensis* that is rare in the Turonian but characteristic of the Coniacian (Pessagno, 1972) and *Multastrum regalis* Vishnevskaya typical of the Coniacian–Maastrichtian, and these forms imply that the assemblage characterizes the late Turonian?–Coniacian interval.

Radiolarian assemblage from Sample 3-3 is diverse in taxonomic aspect (over 50 species). More than one third of the assemblage is represented by taxa, which existed throughout the Late Cretaceous, except for the Maastrichtian sometimes. These are *Pseudoaulophacus lenticulatus* (White), *Stylodictya insignis* Campbell et Clark, *Afens liriodes* Reidel et Sanfilippo, *Amphipyndax stocki* (Campbell et Clark), *Cornutella californica* Campbell et Clark, *Cryptamphorella conara* (Foreman), and *Dictyomitra formosa* Squinabol. The assemblage is lacking index species of Cenomanian (*Dactyliosphaera silviae*) and Turonian (*Alievium superbum*) zones distinguished in the Mediterranean region (O'Dogherty, 1994). Many species of the assemblage are unknown from publications. Of particular interest is presence of *Theocampe* sp. cf. *B. tina* characteristic of the Coniacian–Campanian interval (Sanfilippo and Riedel, 1985), although specimens are imperfectly preserved, and occurrence of *Pseudoaulophacus venadoensis* (Turonian–Coniacian). Species *Multastrum regalis* Vishnevskaya is known from the Coniacian–Campanian interval (Vishnevskaya, 2001), while *Acaeniotyle macrospina* (Squinabol) existed since the Albian until the Turonian. According to results of preliminary taxonomic analysis, we suggest the late Turonian?–Coniacian age for the assemblage based on pres-

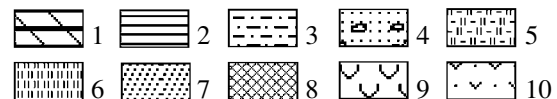
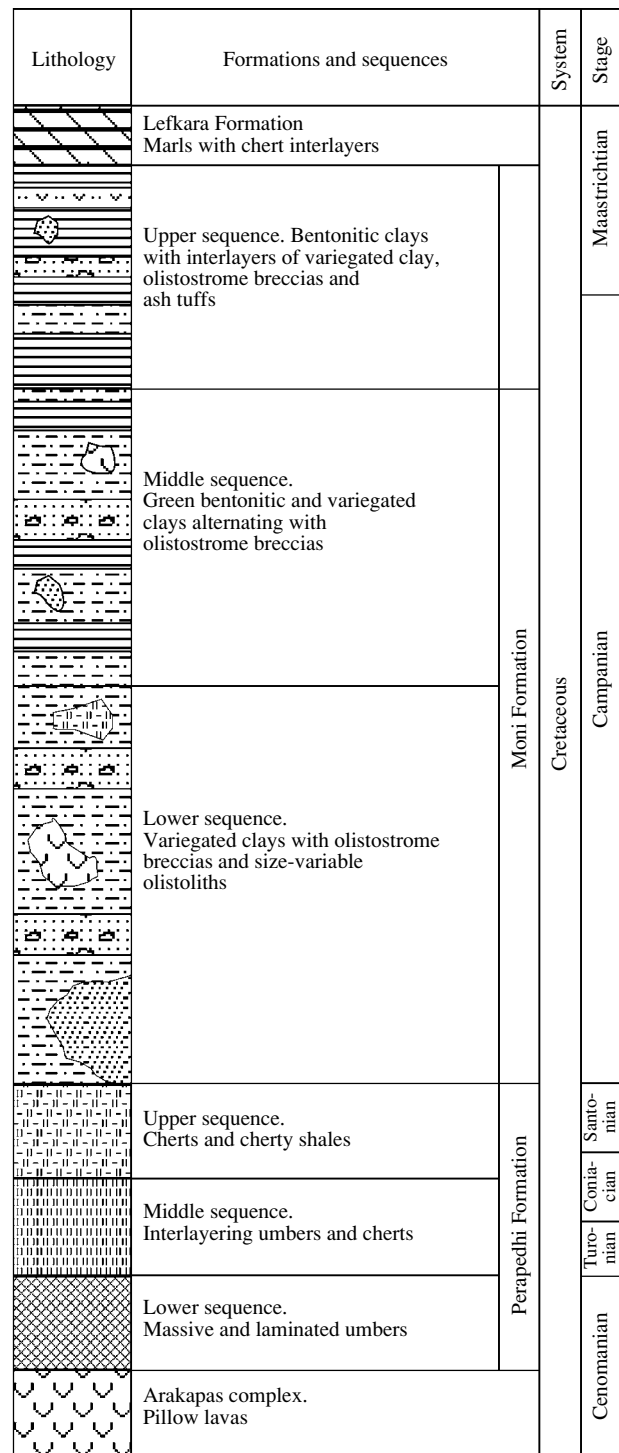
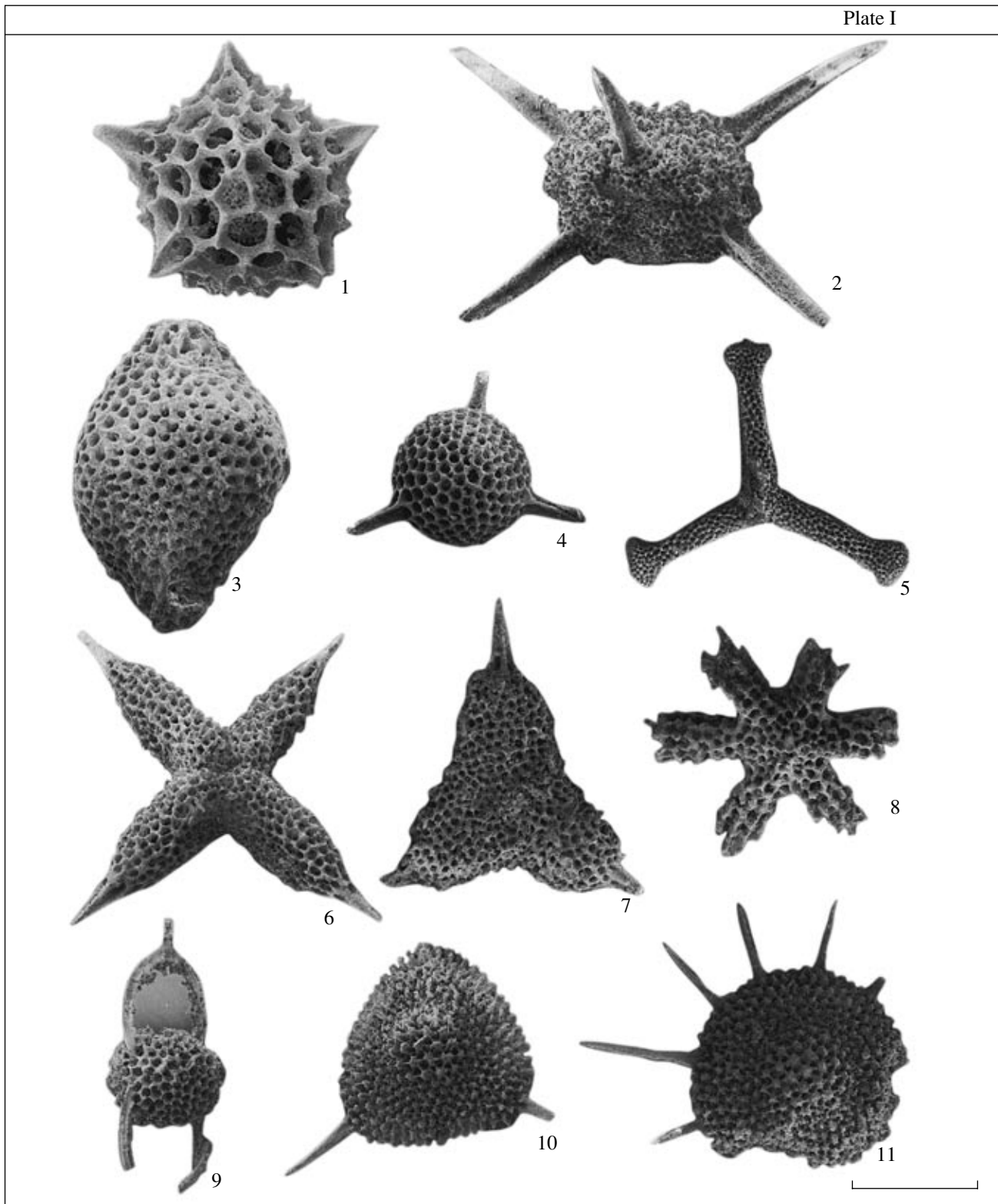


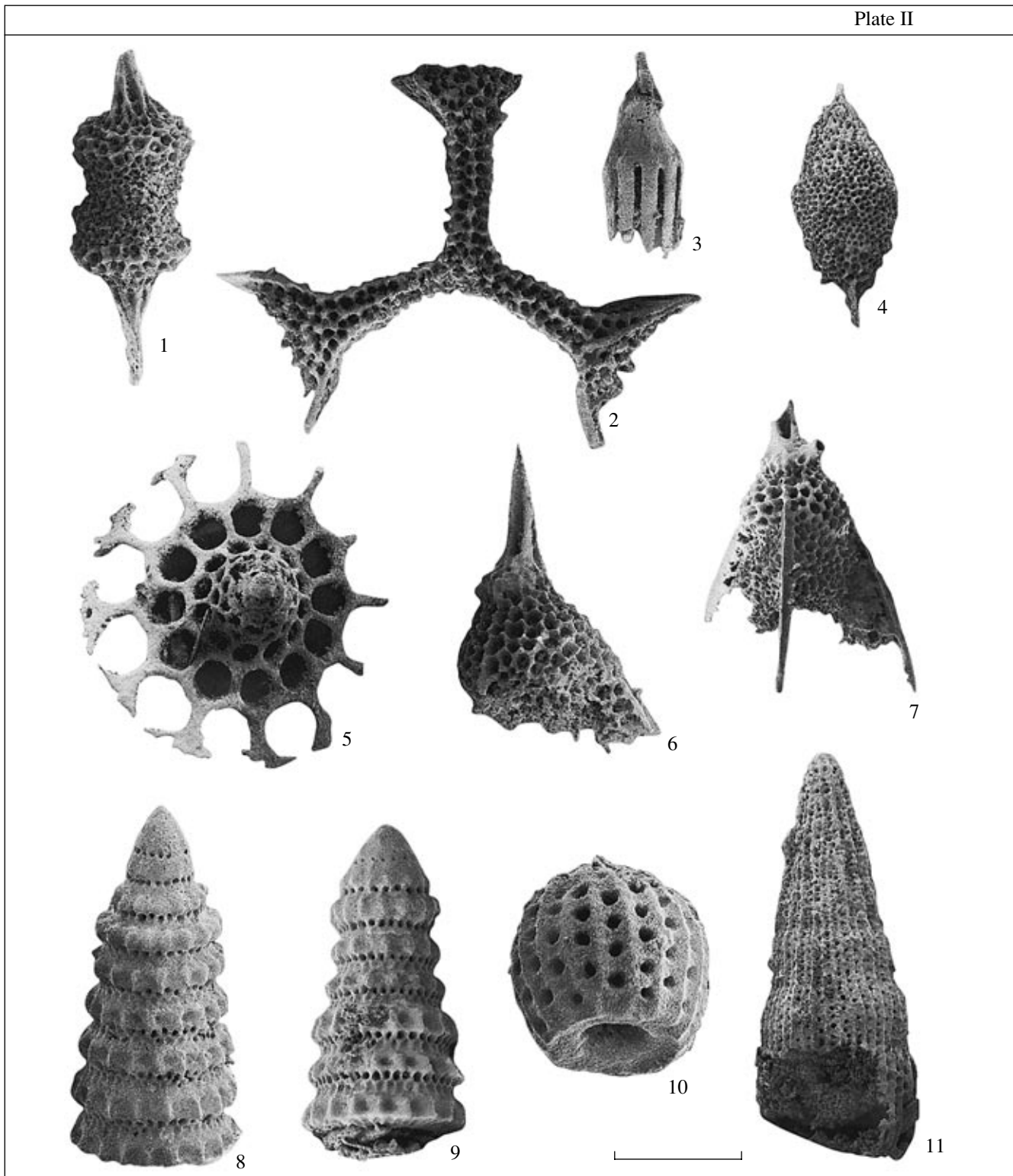
Fig. 6. Composite section of sedimentary cover above the Arakapas ophiolite massif: (1) marl; (2) bentonitic clay; (3) silty clay; (4) olistostrome breccia; (5) opoka-like chert or cherty shale; (6) chert; (7) sandstone; (8) umber; (9) basic volcanics; (10) ashy tuff.

**Plate I.**

(1) *Quinquecapsularia* sp. A; (2) *Acaeniotyle macrospina* (Squinabol, 1903); (3) *Phaseliforma inflata* Bragina, 2004; (4) *Triactoma fragilis* Bragina, 1996; (5) *Patulibracchium* ex gr. *P. teslaensis* Pessagno, 1971; (6) *Crucella messinae* Pessagno, 1971; (7) *Stylodictya insignis* Campbell et Clark, 1944; (8) *Multastrum regalis* Vishnevskaya, 1991; (9) *Vitorfus* sp. A (in Pessagno, 1977); (10) *Alievium* ex gr. *A. murphyi* Pessagno, 1972; (11) *Pseudoaulophacus lenticulatus* (White, 1928).

All specimens are from the middle sequence of the Perapedhi Formation, section 3, Turonian–Coniacian (Sample 3-3). Scale bar is equal to 100 μ m for figs. 1–4, 6–11 and to 200 μ m for fig. 5.

Plate II

**Plate II.**

(1) *Archaeospongoprimum distributum* Bragina, 1996; (2) *Halesium sexangulum* Pessagno, 1971; (3) *Afens liriodes* Riedel et Sanfilippo, 1974; (4) *Distylocapsa squama* O'Dogherty, 1994; (5) *Rotaforma volatilis* O'Dogherty, 1994; (6) *Ultranapora* ex gr. *U. durhami* Pessagno, 1977; (7) *Ultranapora* sp. A; (8) *Pseudodictyomitra nakasekoi* Taketani, 1982; (9) *Pseudodictyomitra* sp. A; (10) *Rhopalosyringium* sp. aff. *R. adriaticum* O'Dogherty, 1994; (11) *Archaeodictyomitra* sp. A.

All specimens are from the middle sequence of the Perapedhi Formation, section 3, Turonian - Coniacian (Sample 3-3). Scale bar is equal to 100 μ m for all the specimens.

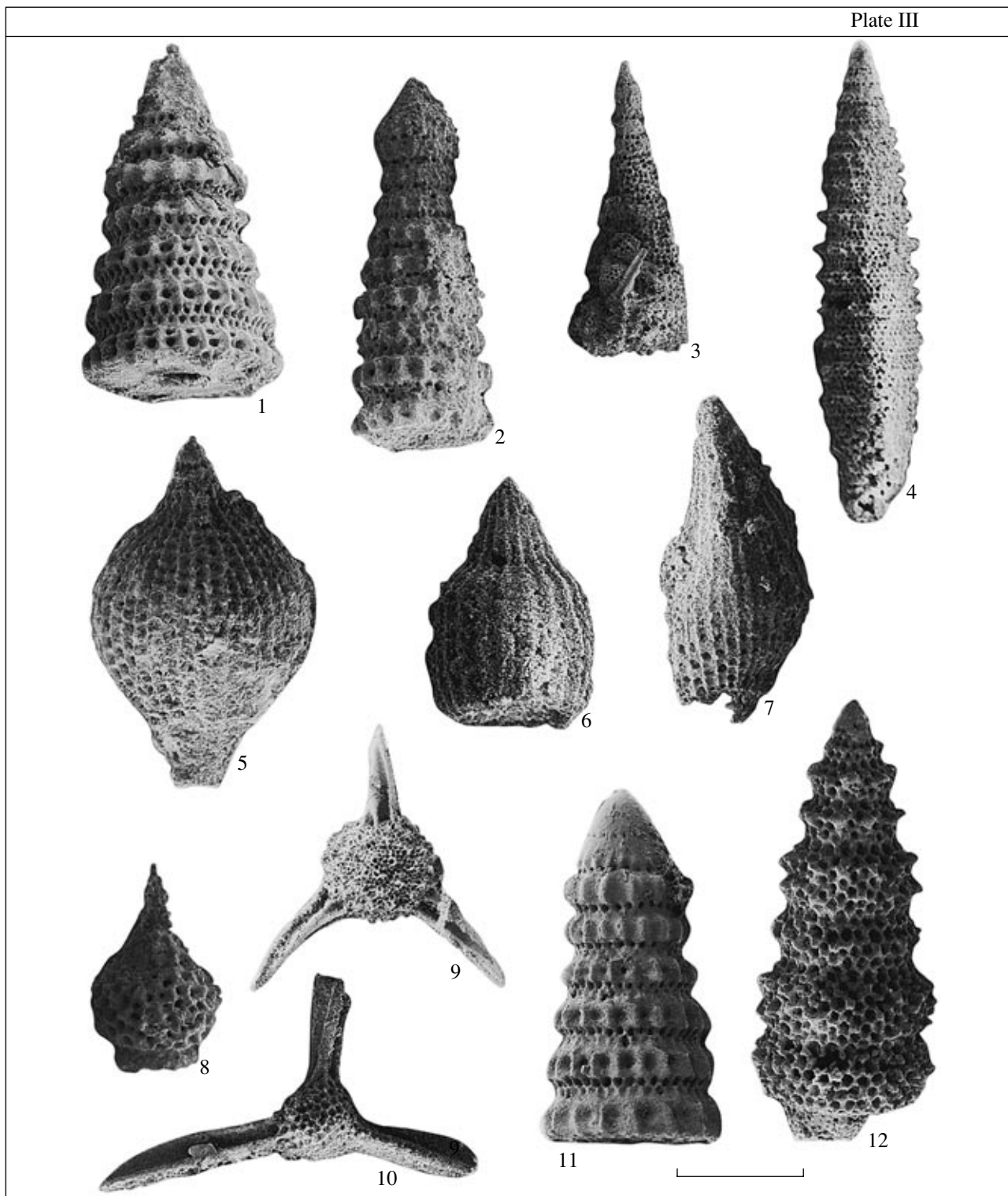


Plate III.

(1) *Pseudodictyomitra* ex gr. *P. nakasekoi* Taketani, 1982; (2) *Pseudodictyomitra pseudomacrocephala* (Squinabol, 1903); (3) *Obelescoites perspicuus* (Squinabol, 1903); (4) *Crolanium spineum* (Pessagno, 1977); (5) *Thanarla spoletensis* O'Dogherty, 1994; (6) *Thanarla pulchra* (Squinabol, 1904); (7) *Dictyomitra obesa* (Squinabol, 1903); (8) *Rhopalosyringium mosquense* (Smirnova et Aliev, 1969); (9) *Acaeniotyle tribulosa* Foreman, 1973; (10) *Triactoma paronai* (Squinabol, 1903); (11) *Pseudodictyomitra* sp. A; (12) *Xitus* sp. A.

(1) middle sequence of the Perapedhi Formation, section 3, Turonian - Coniacian (Sample 3-3); (2–10) Monagroulli Beds, Albian, an olistolith in the Moni Formation, section 56 (Sample 3-2); (11–12) middle sequence of the Perapedhi Formation, section 1, Turonian–Coniacian (Sample 13-1). Scale bar is equal to 100 μ m for figs. 1, 2, 7, 8, 11, 12 and to 200 μ m for figs. 3–5, 9, 10.

ence of *Multastrum regalis* Vishnevskaya, *Pseudoaulophacus venadoensis* Pessagno and *Theocampe* cf. *tina* (Foreman).

Radiolarian assemblage from the upper sequence of the Perapedhi Formation (Section 1, Bed 4, Sample 13-4) consists in general of long-lived species of the Albian–Coniacian interval (Bragina, 2003, 2004; Erbacher, 1994; O’Dogherty, 1994; Pessagno, 1969, 1976, 1977). These are, for instance, *Acaeniotyle diaphorogona* Foreman, *A. macrospina* (Squinabol), *A. umbilicata* (Rust), *Acanthocircus impolitus* O’Dogherty, *Vitorfus campbelli* Pessagno, *Dictyomitra formosa* Squinabol, *Microsciadiocapsa sutterensis* Pessagno, *Mita magnifica* Pessagno, *M. sp. B* (Pessagno, 1977), and *Pseudodictyomitra nakasekoi* Taketani. Nevertheless, the assemblage includes up to 80% of species known from the type locality of the Perapedhi Formation (upper Santonian?–Campanian): *Archaeospongoprimum bipartitum* Pessagno, *Crucella cachensis* Pessagno, *C. messinae* Pessagno, *Multastrum regalis* Vishnevskaya, *Patulibracchium* sp. aff. *P. lawsoni* Pessagno, *Praeocaryomma universona* Pessagno, *Pseudoaulophacus lenticulatus* (White), *Stylosphaera pusilla* Campbell et Clark, *Afens liriodes* Reidel et Sanfilippo, *Annikaella omanensis* De Wever, *Bathropyramis* sp. A, *Cornutella californica* Campbell et Clark, *Dictyomitra formosa* Squinabol, *Mita* sp. A (= *Theocampe* (?) sp. in Bragina and Bragin, 1996), *M. sp. D* (= *Stichomitra* (?) sp. in Bragina and Bragin, 1996), including five species *Archaeospongoprimum distributum* Bragina, *Triactoma fragilis* Bragina, *Stichomitra perapedhia* Bragina, *Theocampe* (?) *cypraea* Bragina, *Theocoronium subtriquetrus* Bragina described from the same deposits (Bragina and Bragin, 1996). *Microsciadiocapsa madisonae* present in the assemblage is of the Turonian–Coniacian age (Pessagno, 1969). *Acanthocircus tympanum* originated in the Turonian (O’Dogherty, 1994; Salvini and Marcucci Passerini, 1998), but we do not exclude that this form existed in the Coniacian as well. Species *Archaeospongoprimum bipartitum* is regarded as characteristic of the Coniacian–Santonian (Pessagno, 1976); *Multastrum regalis* of the Coniacian–Campanian stratigraphic interval (Vishnevskaya, 2001). In addition, the assemblage includes first representatives of the genus *Bathropyramis* characterizing commonly the Santonian–Maastrichtian deposits. According to these data, we suggest the Coniacian–Santonian age of the described assemblage.

Older radiolarians occur in olistoliths confined to the lower part of the Moni Formation (Monagroulli Beds, Section 56, Bed 2) (Plate III). For instance, Sample 3-2 yields species frequently occurring in Albian and Cenomanian deposits: *Pseudodictyomitra pseudomacrocephala*, *Rhopalosyringium euganeum*, *Ultranapora durhami*, *U. praespinifera*, and *U. spinifera*; several other species typical of the Albian (*Acaeniotyle tribulosa*, *Crolanium spineum*, *Dictyomitra obesa*, *T. pulchra*) existed until the initial Cenomanian

time only. One more component of the assemblage is *Thanarla spoletensis*, the index species of synonymous zone established in Italy and Spain within the range of the Albian–basal Cenomanian (O’Dogherty, 1994). Nevertheless, *Rhopalosyringium mosquense* and *Tugurium pagoda*, which terminated their evolution in the Albian, are characteristic components of the assemblage that is lacking *Dactyliosphaera silviae*, the index species of synonymous Cenomanian zone (O’Dogherty, 1994), being therefore of the Albian age. In Sample 3-2a collected nearby, there is encountered species *Dactyliosphaera silviae* in association with *Acaeniotyle glebulosa* and *Rhopalosyringium elegans*, which do not occur above the lower Cenomanian. Consequently, the assemblage of Sample 3-2a is definitely of the early Cenomanian age.

The youngest radiolarian assemblages are confined to the upper sequence of the Moni Formation (Section 7, Bed 6, Sample 6-3; Bed 7, Sample 6-2). Species *Alievium praegallowayi*, *Cromyodruppa concentrica*, *Pentinastrum subbotinae*, and *Pseudoaulophacus pargueraensis* identified in Sample 6-3 are very characteristic of the Coniacian–Campanian deposits in lower and high latitudes (Bragina, 1987, 1994; Empson-Morin, 1984; Kozlova and Gorbovets, 1966; Nakaseko and Nishimura, 1981; Pessagno, 1976). Species known from the Campanian–Maastrichtian interval (Empson-Morin, 1981, 1984; Foreman, 1968; Sanfilippo and Riedel, 1985) are *Archaeodictyomitra lamellicostata*, *Podocapsa* (?) *topferia*, *Lithocampe eureia*, and *Pseudoaulophacus riedeli*. According to its taxonomic composition, the relevant assemblage confidently corresponds in age to the Campanian–basal Maastrichtian and cannot be dated more precisely, as it is lacking index species of the Campanian (*Amphipyndax pseudoconulus*) and upper Campanian–Maastrichtian (*Amphipyndax tylotus*) zones.

In Sample 6-2, *Amphipyndax tylotus* (Foreman, 1966), the index species of synonymous upper Campanian–Maastrichtian zone (Sanfilippo and Riedel, 1985), is found in association with several other species characteristic of the same stratigraphic interval, and radiolarians from this sample correspond in age to the late Campanian–Maastrichtian (early Maastrichtian, most likely). In a parallel section, planktonic foraminifers of the upper Campanian–lower Maastrichtian occur approximately at the same level.

CONCLUSIONS

Based on lithostratigraphic subdivision of the Perapedhi and Moni formations and new biostratigraphic data obtained in the course of this study, we arrived at following conclusions:

1. New data confirm the three-member structure of the Perapedhi Formation sections in the southern flank of the Arakapas massif, where they are divisible into the lower (members of the Cenomanian age presumably),

middle (interlayering umbers and cherts of the Turonian–Coniacian), and upper (opoka-like cherts of the Coniacian–Santonian) sequences. Diachronism of the Perapedhi Formation boundaries is also confirmed: upper horizons of the formation are getting younger to the west of the Arakapas massif up to the Santonian–early Campanian.

2. At the base of the Moni Formation, there is established unconformity, and relevant hiatus spans most likely the Santonian Stage. It is established as well that matrix of the Moni olistostrome contains redeposited radiolarians of the Lower Cretaceous and encloses olistoliths, which are composed of the Perapedhi Formation rocks.

3. According to lithology and identified radiolarian assemblages, the Moni Formation is divided into three sequences. The lower sequence is composed of silty clay enclosing large olistoliths; the middle one of interlayering silty and bentonitic clays with abundant small olistoliths. In the upper sequence of predominantly bentonitic clay with interlayers of chert and ash tuff, olistoliths are relatively rare. Upper horizons of the Moni Formation are of the late Campanian–Maastrichtian age.

4. Based on radiolarians, blocks of basic volcanics and limestones, which occur in the Moni olistostrome, correspond in age to the Upper Triassic. Olistoliths comparable in lithology with the Monagroulli Beds are of the Albian–Cenomanian age according to new biostratigraphic data obtained.

ACKNOWLEDGMENTS

The work was supported by the Russian Foundation for Basic Research, project no. 03-05-64964.

Reviewer V.S. Vishnevskaya

REFERENCES

- Ch. D. Blome and W. R. Irwin, "Equivalent Radiolarian Ages from Ophiolitic Terranes of Cyprus and Oman," *Geology* **13** (6), 401–404 (1985).
- N. Yu. Bragin, L. G. Bragina, and K. A. Krylov, "Albian–Cenomanian Deposits of the Mamonia Complex, Southwestern Cyprus," in *Proceedings of the Third International Conference on the Geology of the Eastern Mediterranean*, Ed. by I. Panayides, C. Xenophontos, and J. Malpas (2000), pp. 309–315.
- L. G. Bragina, "Comparative Analysis of Radiolarian Assemblages from Upper Cretaceous (Santonian) Deposits of the Moscow Region," in *Proceedings of the IX All-Union Seminar on Radiolarians: Radiolarians and Biostratigraphy* (UNTs AN SSSR, Sverdlovsk, 1987), pp. 23–25 [in Russian].
- L. G. Bragina, "Radiolarians and Stratigraphy of the Upper Cretaceous Khot'kovo Group, Moscow Region," *Byull. Mosk. O–va Ispyt. Prir., Otd. Geol.* **69** (2), 91–100 (1994).
- L. G. Bragina, "Cenomanian and Turonian Radiolarians from Crimean Mountains," *Byull. Mosk. O–va Ispyt. Prir., Otd. Geol.* **74** (3), 43–50 (1999).
- L. G. Bragina, Extended Abstract of Candidate's Dissertation in Geology and Mineralogy (GIN RAN, Moscow, 2001).
- L. G. Bragina, "New Radiolarian Species from the Naiba reference Section of the Upper Cretaceous," *Paleontol. Zh.*, No. 3, 25–30 (2003).
- L. G. Bragina, "Cenomanian-Turonian Radiolarians of Northern Turkey and the Crimean Mountains," *Paleontol. J* **38** (2004).
- L. G. Bragina and N. Yu. Bragin, "Radiolarians and Stratigraphy of Campanian–Maastrichtian Deposits in Southwestern Cyprus," *Stratigr. Geol. Korrelyatsiya* **3** (2), 147–155 (1995) [*Stratigr. Geol. Correlation* **3** (2), 147–155 (1995)].
- L. G. Bragina and N. Yu. Bragin, "Stratigraphy and Radiolarians from the Type Section of Perapedhi Formation (Upper Cretaceous of Cyprus)," *Stratigr. Geol. Korrelyatsiya* **4** (3), 38–45 (1996) [*Stratigr. Geol. Correlation* **4** (3), 246–53 (1996)].
- K. M. Empson-Morin, "Campanian Radiolaria from DSDP Site 313, Mid-Pacific Mountains," *Micropaleontol.* **27** (3), 249–292 (1981).
- K. M. Empson-Morin, "Depth and Latitude Distribution of Radiolaria in Campanian (Late Cretaceous) Tropical and Subtropical Oceans," *Micropaleontol.* **30** (1), 87–115 (1984).
- J. Erbacher, "Entwicklung und Palaoozoogeographische mittelkretazischer Radiolarien der westlichen Tethys (Italien) und des Nordatlantiks," *Tubinger Mikropal. Mitt.* Tubingen, No. 12, 1–119 (1994).
- H. Foreman, "Two Cretaceous Radiolarian Genera," *Micropaleontol* **12** (3), 355–359 (1966).
- H. Foreman, "Upper Maastrichtian Radiolaria of California," *Spec. Pap. Paleontol.*, No. 3, 1–82 (1968).
- G. E. Kozlova and A. N. Gorbovets, "Radiolarians from Upper Cretaceous and Upper Eocene Deposits of the West Siberian Lowland," *Tr. VNIGRI*, No. 248, 1–159 (1966).
- M. Mantis, Upper Cretaceous–Tertiary Foraminiferal Zoning in Cyprus: *Trans. Epetiris Cyprus Research Centre, Nicosia*, 227–241 (1970).
- K. Nakaseko and A. Nishimura, "Upper Jurassic and Cretaceous Radiolaria from the Shimanto Group in Southwest Japan," *Sci. Rep. College Gen. Educ. Osaka Univ.* **30** (2), 133–203 (1981).
- L. O'Dogherty, "Biochronology and Paleontology of Mid-Cretaceous Radiolarians from Northern Apennines (Italy) and Betic Cordillera (Spain)," *Mem. Geol. Lausanne*, No. 21, 413 (1994).
- S. Oozawa and M. Okamura, "New Radiolarian Ages from the Troodos Ophiolite and Their Tectonic Implications," *Island Arc* **2** (1), 1–6 (1993).
- T. M. Pantazis, "The Geology and Mineral Resources of the Pharmakas–Kalavassos Area," *Mem. Geol. Survey Cyprus.*, No. 6, 1–120 (1967).
- E. A. Pessagno, Jr., "The Neosciadiocapsidae, a New Family of Upper Cretaceous Radiolaria," *Bull. Amer. Paleontol.* **56** (253), 377–439 (1969).

23. E. A. Pessagno, Jr., "Cretaceous Radiolaria. Part I: The Phaseliformidae, New Family, and Other Spongodiscacea from the Upper Cretaceous Portion of the Great Valley Sequence, Part II; Pseudoaulophacidae Riedel from the Cretaceous of California and the Blake-Bahama Basin (JOIDES Leg I)," *Bull. Am. Paleontol.* **61** (270), 269–328 (1972).
24. E. A. Pessagno, Jr., "Radiolarian Zonation and Stratigraphy of Upper Cretaceous Portion of the Great Valley Sequence," *Micropaleontol.*, No. 2, 1–96 (1976).
25. E. A. Pessagno, Jr., "Lower Cretaceous Radiolarian Biostratigraphy of the Great Valley Sequence and Franciscan Coast Ranges," *Publ. Cushman Found. Foramin. Res.* **15**, 1–87 (1977).
26. G. Salvini and M. Marcucci Passerini, "The Radiolarian Assemblages of the Bonarelli Horizon in the Umbria-Marche Apennines and Southern Alps, Italy," *Cretaceous Res.* **19** (6), 777–804 (1998).
27. A. Sanfilippo and W. R. Riedel, "Cretaceous Radiolaria," in *Plankton Stratigraphy* (Cambridge Univ. Press, New York, 1985), pp. 573–630.
28. K. O. Simonian and I. G. Gass, "Arakapas Fault Belt, Cyprus: a Fossil Transform Fault," *Bull. Geol. Soc. Am.* **89** (8), 1220–1230 (1978).
29. R. E. Swarbrick and A. H. F. Robertson, "Revised Stratigraphy of the Mesozoic Rocks of Southern Cyprus," *Geol. Mag.* **117** (5), 547–563 (1980).
30. E. Urquhart and F. T. Banner, "Biostratigraphy of the Supra-Ophiolite Sediments of the Troodos Massif, Cyprus: the Cretaceous Perapedhi, Kannaviou, Moni and Kathikas Formations," *Geol. Mag.* **131** (4), 499–518 (1994).
31. E. Urquhart and A. H. F. Robertson, "Radiolarian Evidence of Late Cretaceous Exotic Blocks at Mangaleni, Cyprus, and Implications for the Origin and Emplacement of the Related Moni Melange," in *Proc. Third Intern. Conference Geol. East. Mediterranean* (Geol. Survey Dept, Nicosia, 2000), pp. 299–307.
32. V. S. Vishnevskaia, *Radiolarian Biostratigraphy of the Jurassic and Cretaceous in Russia* (GEOS, Moscow, 2001) [in Russian].
33. R. A. M. Wilson, *The Geology of the Xeros-Troodos Area* (Cyprus Geol. Survey Dept., Nicosia, 1959).